Simultaneous measurement of magnetic field and temperature based on magnetic fluid-clad long period fiber grating

J. Tang College of Science, University of Shanghai for Science and Technology, Shanghai 200093, China

S. Pu College of Science, University of Shanghai for Science and Technology, Shanghai 200093, China
shlpu@usst.edu.cn

L. Luo College of Science, University of Shanghai for Science and Technology, Shanghai 200093, China

S. Dong College of Science, University of Shanghai for Science and Technology, Shanghai 200093, China

Simultaneous measurement of magnetic field and temperature is proposed and experimentalized with a magnetic fluid-clad long period fiber grating structure. Magnetic fluid is used as the surrounding material of the long period fiber grating. Both of the wavelength and intensity of the spectral resonance valley of the proposed structure can be influenced by the applied magnetic field and ambient temperature variation. A two-parameter matrix method is proposed and utilized to measure the magnetic field and temperature simultaneously. The linear relationship between the corresponding wavelength shift/intensity variation and magnetic field/temperature change is obtained at certain ranges of magnetic field and temperature, which is favorable for sensing applications.
[DOI: http://dx.doi.org/10.2971/jeos.2015.15025]

Keywords: Magnetic field sensing, temperature sensing, cross-sensitivity, magnetic fluid, two-parameter matrix method

1 INTRODUCTION

Optical fiber sensors have attracted extensive interest over the past decades, which are due to their particular characteristics, such as high sensitivity, low cost and ease of fabrication. Versatile structures have been employed, for example, single-mode-multimode-multimode fiber structure [1], up-tapered joints fiber-optic structure [2]. On the other hand, magnetic fluid (MF) is a kind of intriguing material with the fluidity of liquids and magnetic property of solid magnetic materials, which consists of surfactant-coated ∼10 nm magnetic nanoparticles dispersed in a suitable liquid carrier and has various applications in optical and sensing fields because of its unique magneto-optical effects such as linear birefringence, linear dichroism, Faraday ellipticity and Faraday rotation. Recently, many potential optical and fiber-optic magnetic field sensing applications based on MFs have been proposed. The designed structures including Sagnac interferometer [3], Fabry-Perot Interferometer [4], singlemode-multimode-singlemode fiber structure [5, 6], multimode-singlemode-multimode fiber structure [7], core-offset fiber structure [8, 9], tapered fiber structure [10]–[12], thin-core fiber mode interferometer [13, 14], hollow-core fiber [15] and photonic crystal fiber/waveguide [16]–[18]. Most of the magnetic field sensing structures are based on the interferometric configurations. Due to the large thermo-optical coefficient of MF, the corresponding sensing structures may be sensitive to the ambient temperature variation simultaneously [19, 20], which will affect the magnetic field sensing accuracy and performance. That is to say, the issue of magnetic field and temperature cross-sensitivity occurs for the MF-based fiber-optic magnetic field sensors.

Long period fiber grating (LPFG) operates through the coupling between core and cladding modes. The resonant wavelength of LPFG is highly sensitive to the external surroundings and the ambient temperature. Therefore, LPFG is very suitable for measuring the external surrounding variation (usually refractive index variation) and ambient temperature change. LPFG has been successfully utilized for temperature measurements and compensation [21]–[25]. Considering these, the MF-clad LPFG is proposed to measure magnetic field and temperature simultaneously in this work.

2 EXPERIMENTS AND PRINCIPLES

The LPFG utilized in our experiments is provided by Nanjing π-Lightwave Information Technology Co., ltd. The LPFG period is 608 μm. The core and cladding diameters of the LPFG are around 9 and 125 μm, respectively. The LPFG is put into the capillary filled with MF. The inner diameter of the capillary is about 1 mm. Both ends of the capillary are then sealed with UV glue to avoid MF evaporating or leaking. The water-based Fe_3O_4 MF with saturation magnetization of ∼20 mT and density of 1.18×10^3 kg/m^3 are provided by Beijing Sunrise Ferrofluid Technological Co. The diameter of the magnetic nanoparticles within the MF is around 10 nm. The as-fabricated structure is placed in the magnetic field for ex-

Received February 12, 2015; revised ms. received April 21, 2015; published May 12, 2015 ISSN 1990-2573

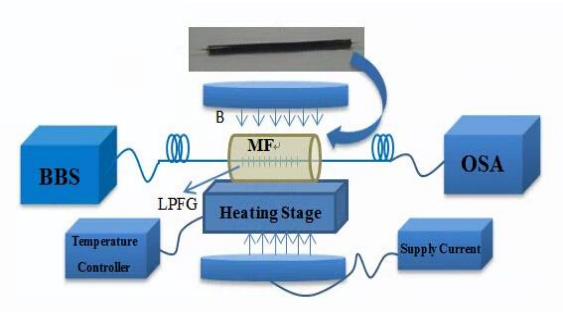

FIG. 1 Experimental setup for investigating the magnetic field and temperature sensing properties of MF-clad LPFG sensing structure.

perimental investigation as shown in Figure 1. The magnetic field is produced by an electrical magnet and its strength can be tuned by adjusting the supply current. The light from the broadband light source (BBS) is coupled into the sensing segment (MF-clad LPFG). The transmitted light is analyzed by an optical spectrum analyzer (OSA). For studying the temperature effect, the sensing segment is put on a heating stage. The ambient temperature around the sensing segment is controlled by the temperature controller.

Under phase matching condition, the resonant wavelength of the LPFG can be written as [26]

$$\lambda_i = \left[n_{core}(\lambda_i) - n^i_{clad}(\lambda_i) \right] \Lambda \ , \tag{1}$$

where λ_i is the i-order mode resonant wavelength, $n_{core}(\lambda_i)$ is the effective index of the core mode, $n^i_{clad}(\lambda_i)$ is the effective index of the i-order cladding mode and Λ is the grating period. It is well-known that MF has unique properties of magnetic-field-dependent refractive index [27]–[29]. When MF is used as the external surrounding of the LPFG, the effective index of LPFG cladding mode will vary with the magnetic field. According to Eq. (1), the LPFG resonant wavelength will vary with the magnetic field as well. Hence, the magnetic field sensing purpose is realized. Besides, the Λ and effective indices of the core and cladding modes will vary with ambient temperature due to the thermal expansion and thermo-optical effects of the LPFG material, respectively. This will lead to the shift of LPFG resonant wavelength with temperature. So, the issue of magnetic field and temperature cross-sensitivity occurs. To fix this issue, a two-parameter matrix method is proposed and utilized in this work.

Under the influence of magnetic field and temperature, the resonant wavelength shift $(\Delta\lambda)$ of the MF-clad LPFG changes as follows

$$\Delta\lambda = K_{\lambda,B} B + K_{\lambda,T} T \ , \tag{2}$$

where B and T are the applied magnetic field and ambient temperature variation, respectively. $K_{\lambda,B}$, $K_{\lambda,T}$ are, respectively, the sensitivities of resonant wavelength shift to magnetic field and temperature. Meanwhile, the depth (viz. transmission loss) of the resonance valley in the transmitted spectrum changes with the magnetic field and temperature. This is assigned to the coupling variation between core and cladding modes. This coupling variation is due to the influence of magnetic field and temperature on the field profiles of LPFG core and cladding modes. As a result, the transmitted intensity variation of the resonance valley (ΔI) can be express as

$$\Delta I = K_{I,B} B + K_{I,T} T \ , \tag{3}$$

where $K_{I,B}$ and $K_{I,T}$ are, respectively, the sensitivities of intensity variation at resonant wavelength to magnetic field and temperature. Combining Eqs. (2) and (3), a well-conditioned system of two equations for $\Delta\lambda$ and ΔI can be given in a matrix form as follows

$$\begin{bmatrix} \Delta\lambda \\ \Delta I \end{bmatrix} = \begin{bmatrix} K_{\lambda,B} & K_{\lambda,T} \\ K_{I,B} & K_{I,T} \end{bmatrix} \begin{bmatrix} B \\ T \end{bmatrix} \tag{4}$$

According to Eq. (4), the strength of magnetic field B and the ambient temperature variation T can be obtained as

$$\begin{bmatrix} B \\ T \end{bmatrix} = \frac{1}{M} \begin{bmatrix} K_{I,T} & -K_{\lambda,T} \\ -K_{I,B} & K_{\lambda,B} \end{bmatrix} \begin{bmatrix} \Delta\lambda \\ \Delta I \end{bmatrix} \tag{5}$$

where $M = K_{\lambda,B}K_{I,T} - K_{\lambda,T}K_{I,B}$ is the determinant of the coefficient matrix. Therefore, by monitoring the wavelength shift ($\Delta\lambda$) and intensity variation (ΔI) at resonant wavelength simultaneously, the measurands (B and T) can be derived from Eq. (5) simultaneously. By this two-parameter matrix method, the issue of magnetic field and temperature cross-sensitivity can be solved in a simple and easy way.

3 RESULTS AND DISCUSSION

The transmission spectra of the MF-clad LPFG structure at magnetic field strength ranging from 0 to 60 mT (at room temperature, i.e. ambient temperature kept at T=20°C) and at ambient temperature ranging from 25 to 70°C (without magnetic field, i.e. B=0 mT) are plotted in Figures 2 and 3, respectively. Figures 2 and 3 imply that both of the depth and wavelength of the resonance valley change with magnetic field (especially at low field regime, i.e. 0-20 mT) and the ambient temperature obviously. This is in agreement with the aforementioned theoretical speculation.

Figures 4 and 5 explicitly show the corresponding wavelength shift and transmission variation of the spectral valley with magnetic field and temperature, respectively. Figures 4 and 5 indicate that the near linear relationships exist at certain ranges of magnetic field and temperature. The magnetic field range of 5-20 mT and temperature range of 25-70°C have been utilized for linear fitting (for the transmission variation, the lowest magnetic field for the linear range goes down to zero). The deviation of the data points from the linear fitting may be assigned to the measurement errors or the intrinsic fluctuation of out spectrum for the MF-based sample, which may be related the Brownian motion and scattering of the magnetic nanoparticles within the liquid carrier. The very slight variation (sensitivity) at low magnetic field is due to the unique magnetic-field-dependent properties of magnetic fluid. It is well-known that the response of magnetic fluid to external magnetic field satisfies the Langevin-like function [9, 30, 31].

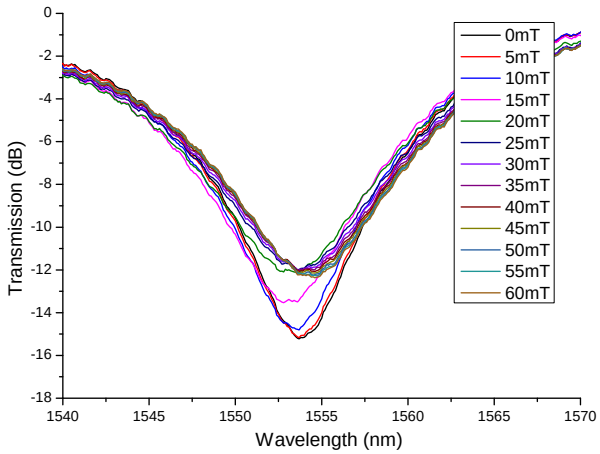

FIG. 2 Transmission spectra of the MF-clad LPFG structure at magnetic field strength ranging from 0 to 60 mT.

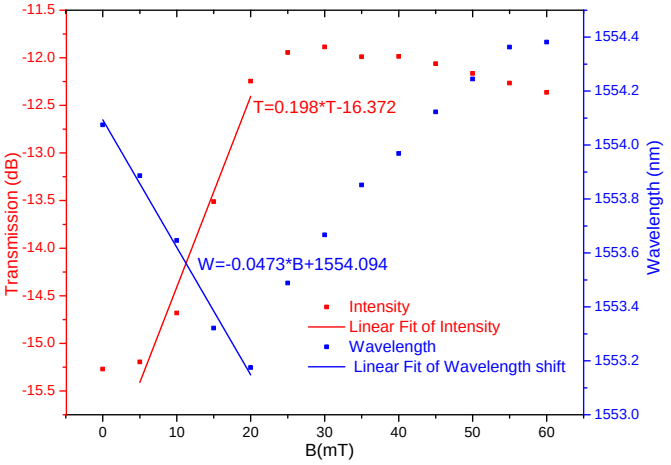

FIG. 4 Resonant wavelength and intensity of the spectral valley at different magnetic field strengths.

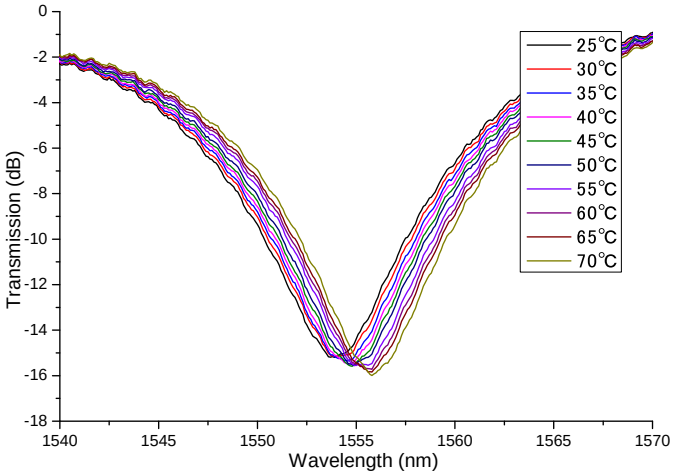

FIG. 3 Transmission spectra of the MF-clad LPFG structure at ambient temperature ranging from 25 to 70°C.

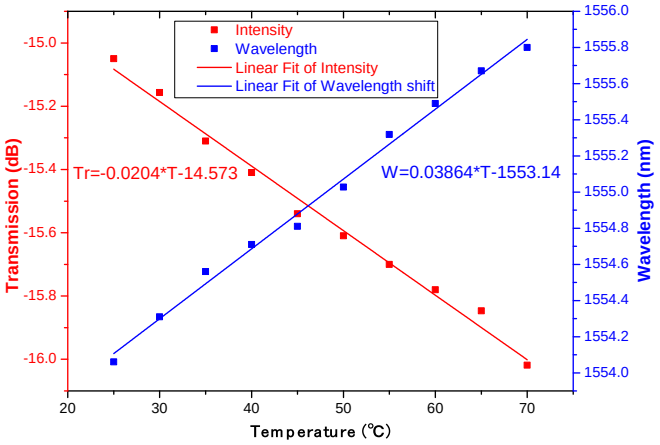

FIG. 5 Resonant wavelength and intensity of the spectral valley at different ambient temperature.

So, this characteristic will limit the application of the proposed sensor at very low magnetic field regime. The slopes obtained from Figures 4 and 5 give the values for $K_{\lambda,B}$, $K_{\lambda,T}$, $K_{I,B}$ and $K_{I,T}$ in Eqs. (2)–(5). Thus, Eq. (5) can now be rewritten in the explicit form

$$\begin{bmatrix} B \\ T \end{bmatrix} = \frac{1}{-0,00668} \begin{bmatrix} -0,0204 & -0,0386 \\ -0,1980 & -0,0473 \end{bmatrix} \begin{bmatrix} \Delta\lambda \\ \Delta I \end{bmatrix} \quad (6)$$

According to Eq. (6), the magnetic field and ambient temperature variation can be measured simultaneously by synchronously monitoring the wavelength shift and intensity variation of the spectral resonance valley of the as-fabricated MF-clad LPFG structure. This provides an easy and convenient means to interrogate the magnetic field and temperature simultaneously with a simple structure, which will assure the sensing accuracy and enhance the performance of the related sensors.

Figure 2 shows that the transmission spectrum of the corresponding structure varies very slightly with the magnetic field at high field regime (25-60 mT). This may be due to the unique physical properties of MF. Under relatively high magnetic field, the agglomeration of magnetic nanoparticles within MF tends to saturate. This characteristic limits the application of the proposed MF-clad LPFG structure under relatively high magnetic field. The shift to long wavelength of the resonant for the magnetic field beyond 20 mT may be ascribed to the influence of polarization as reported in [32].

4 CONCLUSION

In summary, the MF-clad LPFG structure is designed. The magnetic field and temperature sensing properties of the as-designed structure are experimentalized. The variation of wavelength and intensity at spectral resonance valley with the applied magnetic field and ambient temperature is utilized to realize the sensing purpose. Considering these properties, a two-parameter matrix method is proposed to measure the magnetic field and ambient temperature simultaneously. This kind of sensing structure may not be suitable for high magnetic field application due to the saturation of magnetic nanoparticle agglomeration within the MF. On the whole, the proposed sensing structure has the advantages of low-cost, compactness and easiness of fixing the issue of magnetic field and temperature cross-sensitivity.

5 ACKNOWLEDGEMENTS

This work was supported by the Shanghai Natural Science Fund of China (Grant no. 13ZR1427400), the Hujiang Foundation of China (Grant no. B14004) and Shanghai Key Laboratory of Specialty Fiber Optics and Optical Access Networks (Grant no. SKLSFO2014-05).

References

[1] N. Bhatia, and J. John, "Multimode interference devices with single-mode-multimode-multimode fiber structure," Appl. Opt. **53**, 5179–5186 (2014).

[2] Z. Kang, X. Wen, C. Li, J. Sun, J. Wang, and S. Jian, "Up-taper-based Mach-Zehnder interferometer for temperature and strain simultaneous measurement," Appl. Opt. **53**, 2691–2695 (2014).

[3] P. Zu, C. C. Chan, G. W. Koh, W. S. Lew, Y. Jin, H. F. Liew, W. C. Wong, et al., "Enhancement of the sensitivity of magneto-optical fiber sensor by magnifying the birefringence of magnetic fluid film with Loyt-Sagnac interferometer," Sensor. Actuat. B-Chem. **191**, 19–23 (2014).

[4] B. Sun, Y. Wang, J. Qu, C. Liao, G. Yin, J. He, J. Zhou, et al., "Simultaneous measurement of pressure and temperature by employing Fabry-Perot interferometer based on pendant polymer droplet," Opt. Express **23(3)**, 1906–1911 (2015).

[5] H. Wang, S. Pu, N. Wang, S. Dong, and J. Huang, "Magnetic field sensing based on singlemode-multimode-singlemode fiber structures using magnetic fluids as cladding," Opt. Lett. **38, No. 19**, 3765–3768 (2013).

[6] R. Zhang, T. Liu, Q. Han, Y. Chen, and L. Li, "U-bent single-mode-multimode-single-mode fiber optic magnetic field sensor based on magnetic fluid," Appl. Phys. Express **7**, 072501 (2014).

[7] J. Tang, S. Pu, S. Dong, and L. Luo, "Magnetic field sensing based on magnetic-fluid-clad multimode-singlemode-multimode fiber structures," Sensors **14**, 19086–19094 (2014).

[8] J. Wu, Y. Miao, W. Lin, B. Song, K. Zhang, H. Zhang, B. Liu, et al., "Magnetic-field sensor based on core-offset tapered optical fiber and magnetic fluid," J. Opt. **16**, 075705 (2014).

[9] J. Wu, Y. Miao, W. Lin, K. Zhang, B. Song, H. Zhang, B. Liu, and J. Yao, "Dual-direction magnetic field sensor based on core-offset microfiber and ferrofluid," IEEE Photonics Technol. Lett. **26**, 1581–1584 (2014).

[10] S. Pu, and S. Dong, "Magnetic field sensing based on magnetic-fluid-clad fiber-optic structure with up-tapered joints," IEEE Photonics J. **6**, 5300206 (2014).

[11] A. Layeghi, H. Latifi, and O. Frazao, "Magnetic field sensor based on nonadiabatic tapered optical fiber with magnetic fluid," IEEE Photonics Technol. Lett. **26**, 1904–1907 (2014).

[12] Y. Miao, J. Wu, W. Lin, B. Song, H. Zhang, K. Zhang, B. Liu, et al., "Magnetic field tunability of square tapered no-core fibers based on magnetic fluid," J. Lightwave Technol. **32**, 4600–4605 (2014).

[13] J. Wu, Y. Miao, B. Song, W. Lin, H. Zhang, K. Zhang, B. Liu and J. Yao, "Low temperature sensitive intensity-interrogated magnetic field sensor based on modal interference in thin-core fiber and magnetic fluid," Appl. Phys. Lett. **104**, 252402 (2014).

[14] G. Huang, B. Zhou, Z. Chen, H. Jiang, and X. Xing, "Magnetic-field sensor utilizing the ferrofluid and thin-core fiber modal interferometer," IEEE Sens. J. **15**, 333–336 (2015).

[15] B. Song, Y. Miao, W. Lin, H. Zhang, B. Liu, J. Wu, H. Liu and D. Yan, "Loss-based magnetic field sensor employing hollow core fiber and magnetic fluid," IEEE Photonics Technol. Lett. **26**, 2283–2286 (2014).

[16] H. Chen, S. Li, J. Li, and Z. Fan, "Magnetic field sensor based on magnetic fluid selectively infilling photonic crystal fibers," IEEE Photonics Technol. Lett. (2015), article in press.

[17] R. Gao, Y. Jiang, and G. Li, "A sandwich structure for the magnetic field detection with supermodes interference," IEEE Photonics Technol. Lett. **27**, 455–458 (2015).

[18] S. Pu, S. Dong, and J. Huang, "Tunable slow light based on magnetic-fluid infiltrated photonic crystal waveguides," J. Opt. **16**, 045102 (2014).

[19] Z. Zhao, M. Tang, F. Gao, P. Zhang, L. Duan, B. Zhu, S. Fu, et al., "Temperature compensated magnetic field sensing using dual S-bend structured optical fiber modal interferometer cascaded with fiber Bragg grating," Opt. Express **22**, 27515–27523 (2014).

[20] X. Li, and H. Ding, "Temperature insensitive magnetic field sensor based on ferrofluid clad microfiber resonator," IEEE Photonics Technol. Lett. **26**, 2426–2429 (2014).

[21] S. Korposh, S. W. James, S.-W. Lee, and R. P. Tatam, "Temperature and surrounding refractive index insensitive cascaded long period grating chemical sensor," Proc. SPIE **9157**, 91574J (2014).

[22] R. Gao, Y. Jiang, and L. Jiang, "Multi-phase-shifted helical long period fiber grating based temperature-insensitive optical twist sensor," Opt. Express **22**, 15697–15709 (2014).

[23] L. Xian, P. Wang, and H. Li, "Power-interrogated and simultaneous measurement of temperature and torsion using paired helical long-period fiber gratings with opposite helicities," Opt. Express **22**, 20260–20267 (2014).

[24] R. Garg, S. M. Tripathi, K. Thyagarajan, and W. J. Bock, "Long period fiber grating based temperature-compensated high performance sensor for bio-chemical sensing applications," Sensor. Actuat. B-Chem. **176**, 1121–1127 (2013).

[25] J. Huang, X. Lan, A. Kaur, H. Wang, L. Yuan, and H. Xiao, "Temperature compensated refractometer based on a cascaded SMS/LPFG fiber structure," Sensor. Actuat. B-Chem. **198**, 384–387 (2014).

[26] C.-Y. Lin, L. A. Wang, and G.-W. Chern, "Corrugated long-period fiber gratings as strain, torsion, and bending sensors," J. Lightwave Technol. **19**, 1159–1168 (2001).

[27] Y. Zhao, D. Wu, R. Lv, and Y. Ying, "Tunable characteristics and mechanism analysis of the magnetic fluid refractive index with applied magnetic field," IEEE Trans. Magn. **50**, 4600205 (2014).

[28] S. Y. Yang, J. J. Chieh, H. E. Horng, C.-Y. Hong, and H. C. Yang, "Origin and applications of magnetically tunable refractive index of magnetic fluid films," Appl. Phys. Lett. **84**, 5204–5206 (2004).

[29] C.-Y. Hong, S. Y. Yang, H. E. Horng, and H. C. Yang, "Control parameters for the tunable refractive index of magnetic fluid films," J. Appl. Phys. **94**, 3849–3852 (2003).

[30] Y. Zhao, D. Wu and R. Q. Lv "Magnetic field sensor based on photonic crystal fiber taper coated with ferrofluid," IEEE Photonics Technol. Lett. **27**, 26–29 (2015).

[31] W. Lin, Y. Miao, H. Zhang, B. Liu, Y. Liu and B. Song, "Fiber-optic in-line magnetic field sensor based on the magnetic fluid and multimode interference effects," Appl. Phys. Lett. **103**, 151101 (2013).

[32] T. G. Liu, Y. F. Chen, Q. Han, and X. Y. Lv "Magnetic field sensor based on U-bent single-mode fiber and magnetic fluid," IEEE Photonics J. **6**, 5300307 (2014).